

Article

A Practical, Adaptive, and Scalable Real-Time Control Approach for Stormwater Storage Systems

Ruijie Liang , Holger Robert Maier * , Mark Andrew Thyer  and Graeme Clyde Dandy 

School of Architecture and Civil Engineering, University of Adelaide, Adelaide 5005, Australia;
mark.thyer@adelaide.edu.au (M.A.T.)

* Correspondence: holger.maier@adelaide.edu.au

Abstract: Traditionally, urban stormwater infrastructure systems consist of passive infrastructure that is not actively controlled in response to rainfall events. Recently, real-time control (RTC) has been considered as a means to significantly increase the capacity and lifespan of these systems. This paper introduces the target flow control systems (TFCS) approach, which can use real-time control of systems of storages to achieve the desired flow conditions at the locations of interest. The first distinctive feature of this approach is that it does not require calibration to catchment-specific data, unlike existing approaches. This means that the TFCS approach is generally applicable to different catchments and is able to respond to future changes in runoff due to land use and/or climate change. The second distinctive feature is that the approach only requires storage-level information measured in real time with the aid of low-cost pressure sensors. This means that the approach is practical and relatively easy to implement. In addition to the introduction of the novel TFCS approach, a key innovation of this study is that the approach is tested on three case studies, each with different physical configurations and stormwater management objectives. Another key innovation is that the TFCS approach is compared to five RTC approaches, including three of the best-performing advanced approaches from the literature. Comparisons of multiple RTC approaches that consider both performance and practicality across multiple case studies are rare. Results show that the TFCS approach is the only one of the five control approaches analysed that has both the best overall performance and the highest level of practicality. The outcomes highlight the potential of the TFCS approach as a practical RTC approach that is applicable to a wide range of catchments with different stormwater management objectives. By maximizing the performance of existing stormwater storages, the TFCS approach can potentially extend the lifespan of existing infrastructure and avoid costly upgrades due to increased runoff caused by land use and climate change.

Keywords: stormwater management; real-time control; urban flooding; stormwater storage



Citation: Liang, R.; Maier, H.R.; Thyer, M.A.; Dandy, G.C. A Practical, Adaptive, and Scalable Real-Time Control Approach for Stormwater Storage Systems. *Water* **2024**, *16*, 2844. <https://doi.org/10.3390/w16192844>

Academic Editors: Shouhong Zhang, Anita Raimondi and Jun Wang

Received: 27 August 2024

Revised: 25 September 2024

Accepted: 29 September 2024

Published: 7 October 2024



Copyright: © 2024 by the authors. Licensee MDPI, Basel, Switzerland. This article is an open access article distributed under the terms and conditions of the Creative Commons Attribution (CC BY) license (<https://creativecommons.org/licenses/by/4.0/>).

1. Introduction

Traditionally, urban stormwater infrastructure systems consist of passive infrastructure that is not actively controlled in response to rainfall events. However, it has been recognized recently that the capacity and lifespan of these systems can be increased significantly by using real-time control (RTC) [1,2]. This is because RTC can be used to offset and, therefore, balance flows from different parts of the system to reduce the coincidence of hydrographs at critical locations [3]. The ability to achieve this is becoming increasingly important as urbanization, densification, and climate change lead to growing pressure on stormwater systems [4,5]. Maximizing the utilization of existing systems with the aid of RTC could potentially delay or avoid expensive and disruptive infrastructure capacity upgrades. The RTC strategies used to control urban stormwater systems can be generally grouped into two categories: (i) predictive control and (ii) reactive control [6].

Predictive control strategies are generally developed based on knowledge of future rainfall values and are tailored to specific rainfall events using optimization algorithms [3,7,8]. Such strategies usually require high-resolution rainfall forecast information

(for example, temporal patterns of upcoming rainfall events [3,7,8]), which enables them to be tailored to individual events to achieve desired flows at critical locations. However, high-resolution rainfall forecast information is not always available or accurate with current technologies, which is likely to compromise the performance of predictive control strategies significantly. In addition, the required optimization processes could be computationally expensive and might, therefore, not be able to be performed within the relatively short timeframes required for real-time control. This is especially the case if evolutionary algorithms are used to perform the optimization.

Reactive control strategies overcome the disadvantages of predictive control strategies by only requiring information that can be measured in real-time, such as storage levels and flow rates. However, these strategies are generally developed based on a range of ‘design’ or historical rainfall events [9–11], which has the disadvantage of requiring calibration, using either manual [12,13] or formal [9,14] optimization approaches. As a result, it is challenging to apply reactive control strategies to catchments with different physical or climatic properties [13]. In addition, reactive control strategies are generally static [15,16], which means that they either perform poorly or need to be recalibrated in response to changes in land use, climate, and stormwater management objectives.

In order to overcome the need for tuning reactive RTC strategies to specific system conditions, Liang et al. (2022) [17] introduced the target flow control (TFC) approach, which is ‘calibration-free’, as it only requires real-time measurements of storage levels in order to determine the orifice opening that achieves the desired outflow from a storage (e.g., the system capacity, which is generally set equal to the capacity of the downstream stormwater infrastructure). This enables this approach to be applied to any system and under any climatic and hydrological conditions without the need for calibration, making it suitable to respond to changing conditions, such as those resulting from climate change. However, this approach was only presented and demonstrated for a single storage, thereby limiting its applicability to practical settings. This is because, for a single storage, the outflow from that storage corresponds to the flow at the location of interest. Consequently, controlling the outflow from the storage also controls the flow at the location of interest. However, this is not the case when control of a system of storages is used to achieve desired target flows at the location(s) of interest, as the outflows from multiple storages contribute to flows at those locations. Consequently, it is unknown what the target outflow from each individual storage should be to achieve the target flows at the locations of interest. In addition, as the inflows to the storages are likely to be different at different times, the target outflows for each storage are also likely to change over time, rather than being static, as is the case for an individual storage, complicating the problem further.

In order to enable the TFC approach to be applied to systems of storages, the objectives of this paper are the following:

1. To extend the TFC approach of Liang et al. (2022) [17] so that it is applicable to systems of storages that are controlled to achieve desired flow target(s) at downstream locations(s) of interest, rather than just a single storage.
2. To demonstrate the utility of the proposed target flow control systems (TFCS) approach on three diverse case studies from the literature that have different storage configurations (e.g., storages in series and parallel) and management objectives (e.g., restricting maximum flow, minimizing overflow volume, maintaining storage levels between operational boundaries).
3. To compare the performance of the proposed TFCS approach with that of benchmark and best-performing advanced approaches from the literature for the three case studies considered.

A key contribution of this study is that this is the first time a novel RTC approach has been tested on multiple case studies, thereby enabling the broader applicability and generality of the approach to be assessed. This is made possible by the calibration-free nature of the proposed TFCS approach, which enables it to be applied to different case studies with ease. As mentioned previously, this is not the case for other reactive control

strategies, which require calibration to site-specific conditions. This makes it significantly more difficult to apply these approaches to different case studies and is likely to be the reason why novel approaches introduced in previous studies have only been tested on a single case study [8,18,19], making it more difficult to assess their applicability under a wider range of conditions. For example, the approaches proposed by Rimer et al. (2023 [20] and Mullapudi et al. (2020) [18] involve the empirical tuning of hyperparameters, while the technique outlined by Schutze et al. (2018) [21] necessitates the use of empirical control rules to determine release strategies for individual storages.

The remainder of this paper is organized as follows. The theoretical underpinnings and implementation of the proposed TFCS approach (Objective 1) are detailed in Section 2, followed by details of the case study and computational experiments used to demonstrate the utility and assess the relative performance of the approach (Objectives 2 and 3) in Section 3. The case study results are presented in Section 4, followed by discussions in Section 5 and conclusions in Section 6.

2. Materials and Methods

2.1. Problem Statement

Figure 1 shows the conceptual approach used in the proposed TFCS reactive control approach to control outflows at each storage. As part of this process, a desired target outflow ($Q_{i,t}$) is specified at the outlet of each storage i at each control time step t for a system of N storages (i.e., $i = 1, 2, \dots, N$). To ensure that this target outflow is achieved at the i th storage, the following equation [17,22,23] is used in control time step t to adjust the i th storage outlet orifice opening percentage ($O_{i,t}$) based on its corresponding storage level ($H_{i,t}$), which can be measured in real time using low-cost sensors:

$$O_{i,t} = \frac{Q_{i,t}}{C_d A_i \sqrt{2gH_{i,t}}} \quad (1)$$

where C_d is the orifice discharge coefficient, A_i is the area of the outlet orifice for the i th storage, and g is the acceleration due to gravity.

Figure 2 illustrates the relationship between outflows at individual storages and flows at the location of interest. As can be seen in Figure 2a, the specification of the desired storage target outflow ($Q_{i,t}$) at a particular storage is relatively easy if $N = 1$ (i.e., for a system consisting of a single storage), as this is equivalent to the target flow at the locations of interest ($Q_{j,t}^*$, $j = 1, 2, \dots, M$ for M locations of interest in the system) (i.e., $Q_{i,t} = Q_{j,t}^*$), which is generally the capacity of the downstream infrastructure. As a result, the desired storage target outflow ($Q_{i,t}$) does not change over time, provided the target flow at the location of interest is static (see Liang et al., 2022 [17]). Consequently, the previously developed TFC reactive control approach [17] can be used for a system with a single storage.

However, when dealing with systems of storages, the target outflow from an individual storage is generally not the same as the target flow at the locations of interest, as the outflows from multiple storages contribute to the flow at those locations (Figure 2b,c). Consequently, it is not known what the target outflows ($Q_{i,t}$) should be at individual storages to achieve the target flow at the location of interest ($Q_{j,t}^*$). In addition, when dealing with systems of storages, the target outflows for individual storages generally change over time ($Q_{i,t}$) in order to ensure target flows at the locations of interest are achieved in response to time-varying storage levels ($H_{i,t}$). Consequently, the key challenge that needs to be addressed when extending the TFC approach from a single storage to a system of storages (i.e., to the TFCS approach) is to determine what the target outflows for individual storages should be at each time step ($Q_{i,t}$).

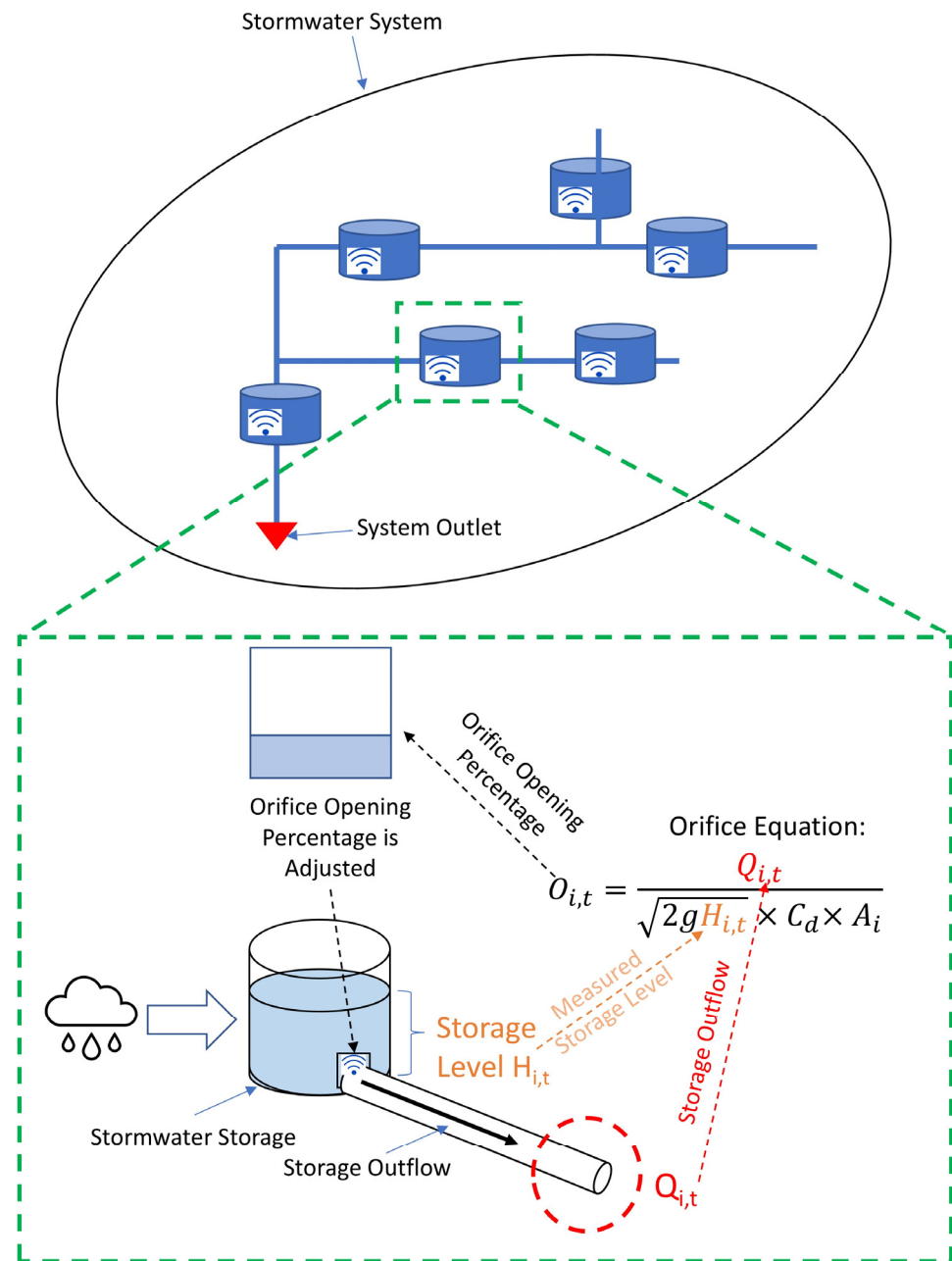


Figure 1. Conceptual approach to controlling outflows at each storage to meet desired target storage outflows used in the proposed TFCS approach, where the orifice equation is used to determine the orifice opening required at time step t to achieve the desired target outflow at that time step for each individual storage in the system. Please note that in the figure, elements related to the flow at the location of interest are represented in “red”, while elements related to storage level are represented in “orange”.

2.2. Proposed Solution

The proposed TFCS approach is only guaranteed to achieve target flows at the location of interest if the available storage capacity at all storages is large enough to detain net inflows (i.e., any inflows in excess of the target outflow) at every time step [17]. Consequently, systems of storages will fail if the available capacity of any of the storages is exceeded at any time step. In order to minimize the chances of this occurring, the target outflows at individual storages at each control time step ($Q_{i,t}$) are selected to be proportional to the ratio of the actual storage volume ($V_{i,t}$) to the maximum storage volume ($V_{i,t}^{max}$) for

each storage (termed the filling degree of the storage, $F_{i,t}$) at each time step, as given in Equation (2) below. This will ensure that the filling degree for each storage is approximately equal at each time step.

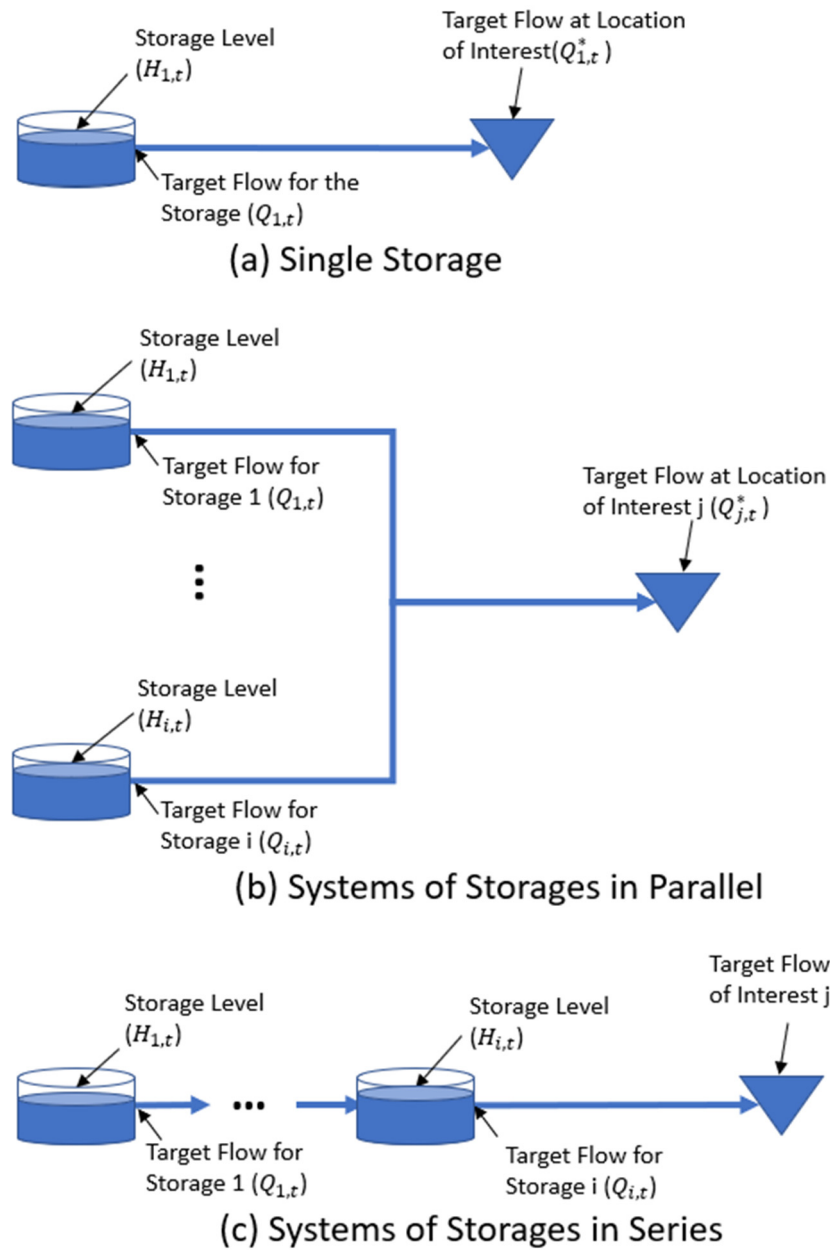


Figure 2. Illustration of the relationship between outflows at individual storages and flows at the location of interest for (a) a single storage (a) and systems of storages with different configurations (i.e., systems of storages in parallel (b) and systems of storages in series (c)).

At each time step:

1. For each storage ($i = 1, \dots, N$), we express the net outflow ($Q_{i,t}^{net}$) to be proportional to its filling degree ($F_{i,t}$) with coefficient K_t :

$$Q_{i,t}^{net} = K_t \times F_{i,t} \text{ for } i = 1, \dots, N \tag{2}$$

where

- a. $Q_{i,t}^{net}$ is the net outflow of storage i at time t , which is the difference between the storage inflow and the unknown target storage outflow ($Q_{i,t}$):

$$Q_{i,t}^{net} = Q_{i,t} - (\sum I_{p,i} \times Q_{p,t}) \text{ for } i = 1, \dots, N \ \& \ p = 1, \dots, N - 1 \tag{3}$$

where $I_{p,i}$ is a system configuration parameter that depends on the storage system layout in the vicinity of each individual storage, such that for storage i and the other storages p ($p = 1, \dots, N - 1$) in the system:

$$I_{p,i} = \begin{cases} 1, & \text{Storage } p \text{ outflow flows into storage } i \\ 0, & \text{Otherwise} \end{cases} \tag{4}$$

- b. $F_{i,t}$ is the filling degree of storage i at time t (i.e., the ratio of the actual storage volume ($V_{i,t}$) at time t to the maximum storage volume ($V_{i,max}$), where the actual storage volume ($V_{i,t}$) is a function of storage level ($H_{i,t}$):

$$F_{i,t} = \frac{V_{i,t}}{V_{i,max}} \tag{5}$$

- c. K_t is the coefficient of proportionality
- 2. We express the flow at the location of interest ($Q_{j,t}^*$) as the sum of the target outflows from the storages ($Q_{i,t}$) that directly contribute to the flow at target location j as follows:

$$\sum I_i^* \times Q_{i,t} = Q_{j,t}^* \text{ for } i = 1, \dots, N \tag{6}$$

where I_i^* is a system configuration parameter that depends on the storage system layout in the vicinity of the location of interest j , such that for the location of interest j and any storage i ($i = 1, \dots, N$) in the system:

$$I_i^* = \begin{cases} 1, & \text{Storage } i \text{ outflow flows into the location of interest } j \\ 0, & \text{Otherwise} \end{cases} \tag{7}$$

- 3. We solve the resulting set of $2N + 1$ linear equations (i.e., Equations (2), (3) and (6)) for the $2N + 1$ unknowns: (1) target outflows at each of the N storages ($Q_{i,t}$, $i = 1, \dots, N$), (2) net outflow at each of the N storages ($Q_{i,t}^{net}$, $i = 1, \dots, N$), and (3) the coefficient of proportionality (K_t') for each timestep t .

Examples of the formulation of Equations (2), (3) and (6) for a number of different example storage configurations are given in Figure 3 for the sake of illustration. The above formulation is able to cater to a broad range of management objectives, including those related to target flows at the location of interest, as well as those related to individual storage capacities, such as maintaining storage levels and minimizing overflows. However, the formulation assumes that travel times between control points and location(s) of interest are small and that the only storage inflows are from sources for which flows are known, which generally corresponds to inflows from other storages.

It should be noted that the above approach belongs to the class of equal filling degree approaches, which have been used to balance the available capacity (filling degree) of systems of storages in previous studies [24,25]. However, existing equal filling degree approaches do not provide a generic method for determining the target outflows of individual storages for networks with different configurations. For example, the approaches suggested by Rimer et al. (2023) [20] and Mullapudi et al. (2020) [18] require the empirical calibration of hyperparameters, and the approach presented by Schutze et al. (2018) [21] requires the application of empirical control rules in order to determine releases at individual storages. As a result, these approaches are not generally applicable to different catchments, system configurations, and management objectives. In addition, existing approaches are static. Therefore, they are not able to respond to changing system conditions, including both

short-term changes during storm events and long-term changes due to climate change. The TFCS approach proposed in this paper overcomes these limitations by presenting a generic formulation that is applicable to any system configuration and can be solved explicitly and efficiently using a wide range of existing approaches, from simple Gauss elimination methods to more complex Jacobi, Gauss–Seidel, and Kaczmarz methods [26,27].

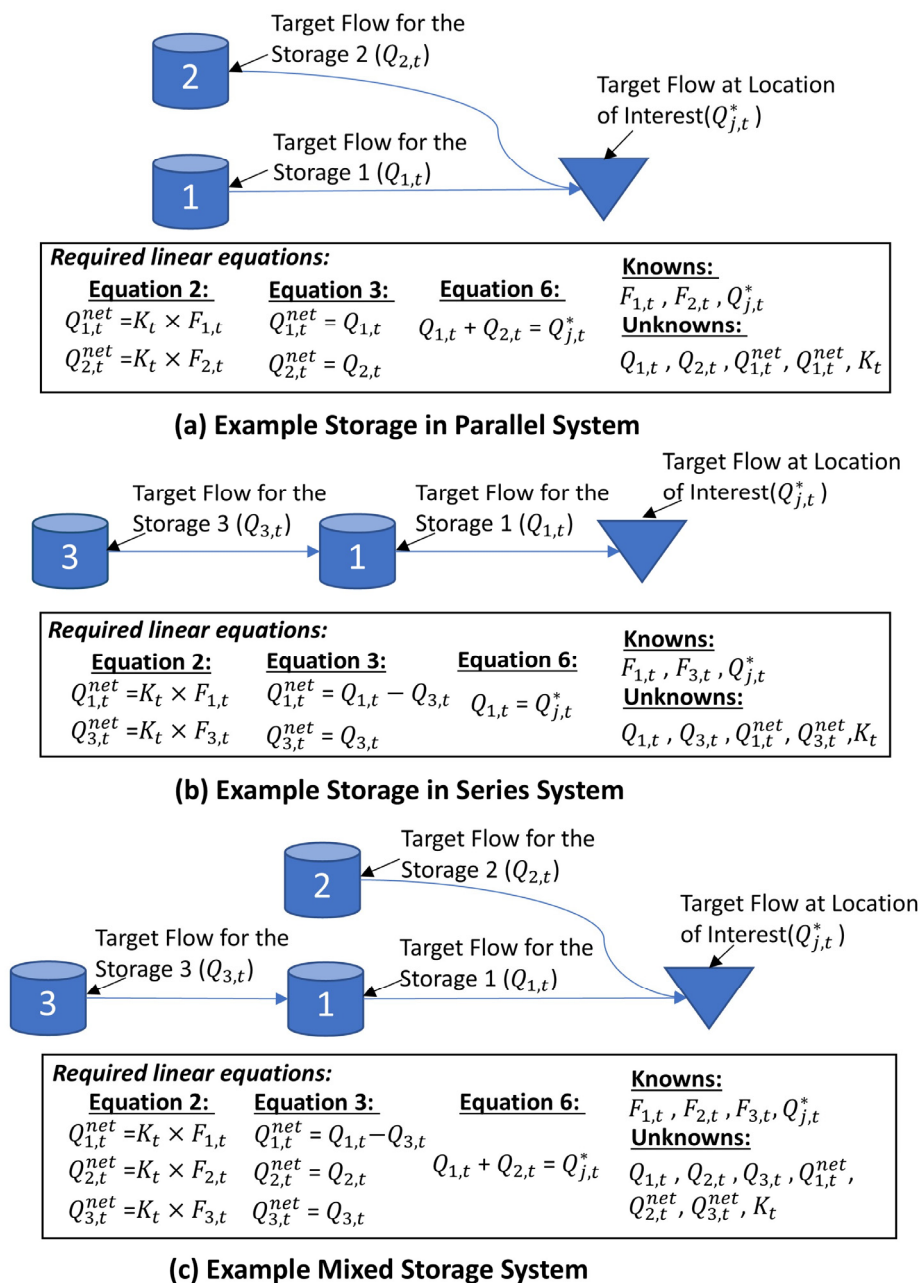


Figure 3. Examples of required linear equations (Equations (2), (3) and (6)) for (a) example storages in parallel system, (b) example storages in series system, and (c) example storages in mixed system (storages in parallel and in series).

2.3. Implementation

The process for implementing the TFCS approach is summarized in Figure 4. The first step is to formulate the set of linear equations (Equations (2), (3) and (6)) that need to be solved in order to obtain the individual target outflows for each of the storages ($Q_{i,t}$) based on the actual system configuration (e.g., number of storages and whether they are in parallel or in series), as detailed in Section 2.2 (Step 1, Figure 4). Next, at any time step t ,

the storage levels ($H_{i,t}$) need to be measured in real time with the aid of pressure sensors placed in the storages (Step 2, Figure 4). The filling degree of each storage ($F_{i,t}$) can then be calculated based on the actual storage volume ($V_{i,t}$, which is a function of measured storage level ($H_{i,t}$)) and corresponding storage capacity in accordance with Equation (3)) (Step 3, Figure 4). After that, the set of $2N + 1$ equations (Equations (2), (3) and (6)) can be solved for the unknown target outflows at each storage ($Q_{i,t}$) using an appropriate solver, such as the Jacobi method [27,28] (Step 4, Figure 4). The orifice opening percentage required at each storage ($O_{i,t}$) to achieve the corresponding target outflow ($Q_{i,t}$) can then be calculated using Equation (1) (Step 5, Figure 4). This process is repeated for the next time step and so on.

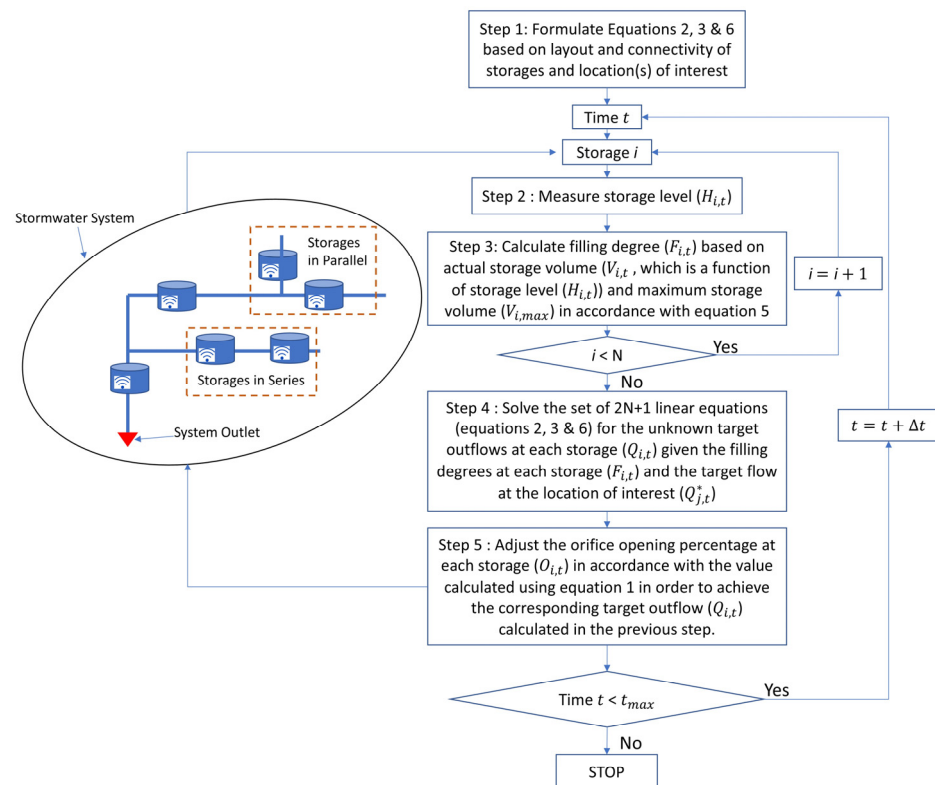


Figure 4. Implementation of the proposed TFCS approach. The inset in the black oval represents the generic illustration of a system of storages from Figure 1.

3. Case Study and Computational Experiments

In order to assess the effectiveness of the proposed TFCS approach for realistic multi-storage systems in a simulated environment, three case studies with different configurations and stormwater management objectives are selected from the literature, the details of which are given in Section 3.1. Details of the computational experiments are given in Section 3.2.

3.1. Case Study and Performance Assessment

3.1.1. Case Study Configuration

Three realistic multistorage case studies are selected to test the effectiveness of the proposed TFCS approach, with the details summarized in Table 1. These case studies are selected due to their high complexity, realism, and diversity, which makes them representative of real storage systems. The storage layouts of the case studies are shown in Figure 5.

Case Study 1 (Gamma) (Figure 5a) is a stormwater system inspired by an urban watershed in Ann Arbor, MI, USA (Case Study no. 1, Table 1). This case study utilizes a total of 11 stormwater storages to control the runoff from 400 hectares of an urbanized catchment (Figure 5a). Four of these storages, which are in series, are controlled using

controllable gate valves with a maximum opening area of 1 m². The objectives are to keep the outflow from storages 1, 2, 3, and 4 below a threshold of 0.14 m³/s [18] and to keep the storage levels at each of the storages below their maximum. Runoff is driven by a 1 in 25 year, 6 h storm event (Table 1), and uniform rainfall is assumed due to the small catchment area [18,20]. The stormwater management model (SWMM) for this case study was provided in previous studies [20].

Table 1. Case study characteristics.

Case Study No.	Name	Catchment Area	Storage Information			Rainfall Information	Objective
			Controlled	In Series	In Parallel		
1	Gamma	400 ha	4	4	0	1 in 25 years, 6 h event	Flow below threshold
2	Astlingen	177 ha	4	2	3	1 year of continuous	Minimize total overflow volume
3	Delta-M	250 ha	5	4	2	48 h obs. event (return period of 2 months)	Storage level within the operational boundary

Case Study 2 (Astlingen) (Figure 5b) is a benchmark urban stormwater network developed by the German Water Association (DWA) (Case Study no. 2, Table 1). The Astlingen network consists of a mixture of combined and separate stormwater systems to reflect realistic conditions in Central Europe. This case study utilizes six storages with a total volume of 5900 m³ to control flows in a catchment with an area of 177 hectares (Figure 5b). Four of the storages (storages 2, 3, 4, and 6) are controlled, including three storages in parallel (storages 2, 3, and 4) and two storages in series (storages 3 and 6). The objective is to minimize the total overflow volume from the storage tanks and overflow structures (Table 1). Spatially variable rainfall information is provided by the four rain gauges located in the Astlingen catchment. One year of continuous historical rainfall data with 5 min resolution is provided for the simulation (Table 1).

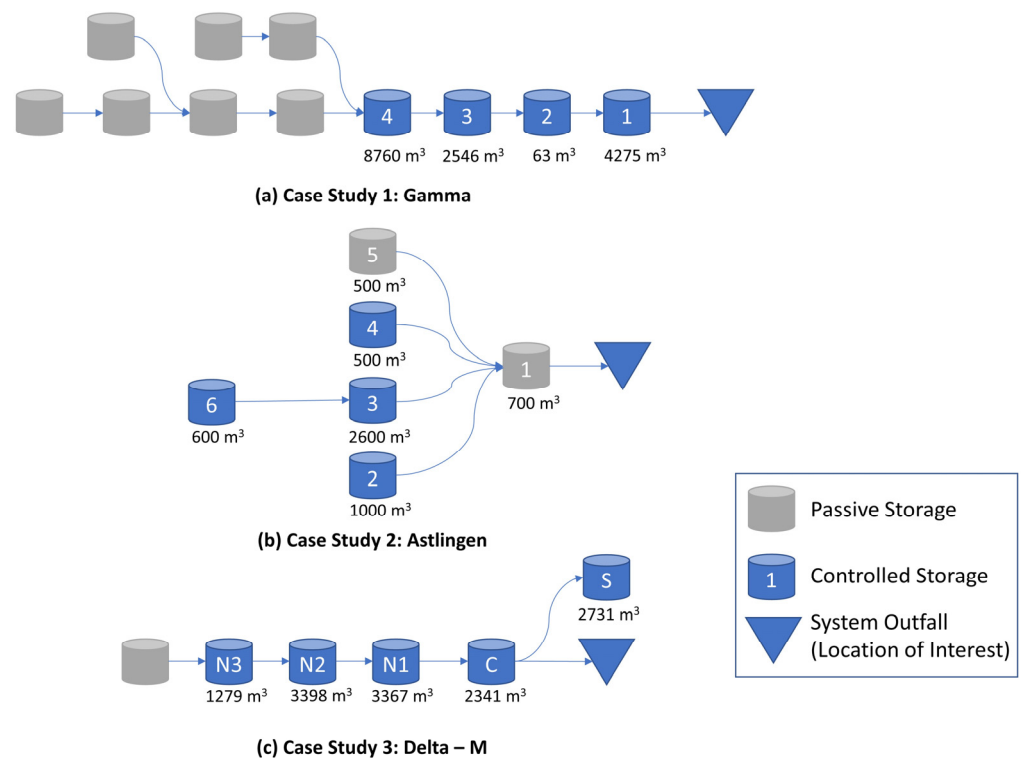


Figure 5. Storage network topology and sizes for the selected case studies: (a) Gamma, (b) Astlingen and (c) Delta-M.

Case Study 3 (Delta-M) (Figure 5c) is a slightly modified version of the Delta case study introduced by Rimer et al. (2023) [20] (Case Study no. 3, Table 1). The Delta case study consists of a combined urban stormwater network with six storages that are located in a residential neighbourhood in order to control flows in a catchment with an area of 250 hectares (Figure 5c). Five of the six storages are controllable, including four storages in series (storages N3, N2, N1, and C) and two storages in parallel (storages C and S). The objective of this case study is to maintain all storage levels within upper and lower thresholds for water quality and aesthetic objectives. Runoff is driven by a 48 h observed storm event with an approximate return period of 2 months that is spatially uniform over the catchment (Table 1). The modifications made to the Delta case study in this paper are to move the location of some of the controllers so that they are directly downstream of the outlets of the active storages, resulting in the Delta-M case study.

3.1.2. Quantitative Performance Assessment

As the objectives of the three selected case studies are different (see Table 1), different metrics are used for assessing the performance of the TFCS approach and the benchmark control approaches (see Table 2). For Case Study 1, the percentage of time each storage exceeds the threshold is used (second row, Table 2), which corresponds to the sum of timesteps the threshold for all storages in the system is exceeded ($\sum_1^N T_{exceed,i}$) compared to the total number of timesteps ($\sum_1^N T_i$). Reduction in total overflow volume is used as the metric for Case Study 2 (third row, Table 2), which corresponds to the difference in total overflow volume (i.e., the overflow volume of all storage in the system for the entire time period, $\sum_1^T (\sum_1^N V_{i,t})$) compared with the ‘No Control’ baseline scenario ($V_{Baseline}$). Case Study 3 (Delta-M) requires two metrics to assess the ability to keep storage levels within their required upper and lower bounds (fourth row, Table 2): (i) the percentage of time outside of the operational boundary, which corresponds to the sum of time outside of the boundary for all storages in the system ($\sum_1^N T_{exceed,i}$) compared to the total time ($\sum_1^N T_i$) and (ii) total deviation of storage levels, which corresponds to the sum of differences between the storage level (H_i) and operational boundaries (upper level: H_{upper} and lower level: H_{lower} ; see Table 2 summed over all storages).

Table 2. Summary of metrics.

Case Study	Objective	Metric
Case Study 1 (Gamma)	Keep flow below the threshold.	a. Percentage of time exceeds threshold: $Time (\%) = \frac{\sum_1^N T_{exceed,i}}{\sum_1^N T_i} \times 100\%$
Case Study 2 (Astlingen)	Minimize overflow volume.	b. Percentage reduction in total overflow volume: $Reduction (\%) = \left(1 - \frac{\sum_1^T (\sum_1^N V_{i,t})}{V_{Baseline}} \right) \times 100\%$
		c. Percentage of time outside of the boundary: $Time (\%) = \frac{\sum_1^N T_{exceed,i}}{\sum_1^N T_i} \times 100\%$
Case Study 3 (Delta-M)	Keep storage level within upper and lower threshold.	d. Total deviation of storage level from operational boundary: $Deviation (m) = \sum_1^T (\sum_1^N (f(H_i, t)))$ where: $f(H_{i,t}) = \begin{cases} H_{i,t} - H_{upper}, & H_{i,t} > H_{upper} \\ 0, & H_{lower} \leq H_{i,t} \leq H_{upper} \\ H_{lower} - H_{i,t}, & H_{i,t} < H_{lower} \end{cases}$

3.2. Computational Experiments

In order to assess the utility of the proposed TFCS approach in absolute terms (Objective 2), its performance is compared with that obtained when there is no outlet control (i.e.,

the storage outlet is always set as fully open). The results of this assessment are provided and discussed in Sections 4.1 and 4.2.

In order to assess the utility of the TFCS approach in relative terms (Objective 3), its performance is compared with that obtained using an equal filling degree (EFD) approach that requires calibration (Section 3.2.1) and the best-performing advanced approaches that have been applied to the three case studies considered in previous studies (Section 3.2.2). Details of the application of the TFCS approach to the case studies are given in Section 3.2.3. The results of the comparison of the TFCS, calibrated EFD, and best-performing advanced approaches are presented and discussed in Section 4.3.

3.2.1. Calibrated EFD Approach

As described previously in Section 2.1, equal filling degree (EFD) approaches that require calibration are used widely for the real-time control of stormwater storages in the literature. Consequently, they provide an excellent benchmark against which to compare the performance of the proposed TFCS approach, which does not require calibration.

The calibrated EFD approach used for comparison in this paper requires calibration of hyperparameters to achieve the balancing of filling degrees [20,25]. Such an approach has already been applied to Case Studies 1 and 2 in previous studies [18,21], enabling the results of these studies to be used as a basis of comparison for the proposed TFCS approach. As a calibrated EFD approach has not been applied to Case Study 3 previously, this was performed as part of this study, using a genetic algorithm [29] to identify the optimal hyperparameters. The hydraulics of the case study system are simulated using EPA SWMM v5.1.012 [30], and the optimization is performed using DEAP (Distributed Evolutionary Algorithms in Python v1.3.0 [31]).

3.2.2. Best-Performing Advanced Approaches

In previous papers, Case Studies 1 and 2 were used to illustrate the utility of novel RTC approaches for systems of stormwater storages [18,19]. The approaches used in each of these papers were different and are currently the best-performing approaches for these case studies. Consequently, the performance of these advanced approaches provides the most rigorous benchmark against which to assess the performance of the proposed TFCS approach for these two case studies.

The advanced approach applied to Case Study 1 is based on reinforcement learning (RL) and uses deep neural networks to train RL-based controllers [18]. In this training process, the RL-based controllers interact with the storage system for thousands of simulated storm scenarios.

The advanced approach applied to Case Study 2 uses model predictive control (MPC) with the assumption of perfect knowledge of future rainfall information at a 5 min sampling interval [19]. The MPC consists of receding horizon optimization with the aid of a simplified conceptual model of the Case Study 2 system.

As an advanced approach has not been applied to Case Study 3 previously, and the optimized predictive control (OPC) approach of Liang et al. (2021) [8] has been proven to be the best-performing algorithm in previous studies [3,7,8], OPC is applied to this case study to provide results from an advanced control approach to act as a benchmark against which to assess the performance of the TFCS approach in a rigorous fashion. This predictive control approach uses an evolutionary algorithm to optimize RTC strategies under the assumption of perfect future rainfall information. For Case Study 3, the following objectives are considered as part of a multiobjective optimization approach: (1) to minimize the time period during which the storage level criteria are violated (i.e., the time period during which storage levels are outside the required operational boundary—see Table 2, Metric c), and (2) to minimize the total deviation of storage level from the operational boundary (i.e., the sum of differences between the storage level and operational boundaries—see Table 2, Metric d). The hydraulics of the case study system are simulated using EPA SWMM v5.1.012 [30], and the optimization is performed using DEAP (Distributed Evolutionary

Algorithms in Python [31]). The optimization process is repeated from three random starting positions in the solution space, and the hypervolume [32–34] of the two objectives is used as an indicator to ensure that the optimization algorithm has converged.

3.2.3. TFCS Approach

The TFCS approach is applied to each of the three case studies following the procedure in Figure 4. Details of Equations (2), (3) and (6) for the three case studies are given in Appendix A. These are solved using the LU decomposition and implemented by using the NumPy Python package. The target flow at the location of interest ($Q_{i,t}^*$) of Case Study 1 is determined based on the objective, which is to keep flow below a threshold. For Case Studies 2 and 3, the target flow at the location of interest ($Q_{i,t}^*$) is determined based on the constraints on the system capacity (maximum flow capacity). The hydraulics of the three case study systems are simulated using EPA SWMM v5.1.012 [30], and the PySWMM wrapper for SWMM v0.5.1 [35] is used to automatically adjust the orifice opening percentages in accordance with the proposed TFCS approach in SWMM.

4. Results

4.1. Overview of Results: Performance of the TFCS Approach

Table 3 shows the performance of the proposed TFCS approach compared with that of the ‘No Control’ scenario, for which the storage outlet is always set as fully open for the three case studies described in Section 3.1. As expected, the TFCS approach always outperforms the ‘No Control’ scenario. In Case Study 1 (second column, Table 3), for the ‘No Control’ scenario, the storage outflow exceeds the target threshold for 47% of the total time, while when using the TFCS approach, this number is decreased to 0%. In Case Study 2 (third column, Table 3), the TFCS approach is able to achieve a 13.2% reduction in total overflow volume compared to the ‘No Control’ scenario. In Case Study 3 (fourth column, Table 3), for the ‘No Control’ scenario, the storage level is outside of the operational boundary for 75.8% of the total time, with a total storage deviation of 687.6 m. For the TFCS approach, the storage level is only outside the operational boundary for 3.2% of the time, and the total storage level deviation is reduced to 0.3 m. These results show that the TFCS approach achieves significant performance improvement compared to the ‘No Control’ scenario for a range of case studies and different stormwater management objectives. Details of the mechanisms causing these improvements in performance when the TFCS approach is used are given in Section 4.2.

Table 3. Performance of TFCS approach.

Control Approach	Case Study 1	Case Study 2	Case Study 3	
	Time (%) *	Reduction (%) **	Time (%) ***	Deviation (m) ****
No Control	47%	0.0%	75.8%	687.6 m
TFCS	0%	13.2%	3.2%	0.3 m

Notes: * Percentage of time flow exceeds the threshold; ** Percentage reduction in total overflow volume; *** Percentage of time storage levels are outside of the operational boundary; **** Total deviation of storage levels.

4.2. Analysis of Results: Illustration of Typical Performance for the TFCS Approach

Figure 6 compares the performance of the proposed TFCS approach with that of the ‘No Control’ scenario using the combined storage system of Case Study 2 as an illustrative example to demonstrate the mechanism by which the TFCS approach improves performance compared with the ‘No Control’ scenario. For this case study, five storages are included in the analysis, including storages in both series and parallel. Storages 2, 3, and 4 are in parallel, feeding storage 1 (Legend and Network Topology, Figure 6). Storage 6 is in series with and upstream of storage 3. Storages 2, 3, 4, and 6 are equipped with control devices, while storage 1 is a passive storage with a static outlet. In order to clearly show the impact of the TFCS approach, the inflows (Figure 6a,b), filling degrees (Figure 6c,d), and

orifice opening percentages (Figure 6e,f) of individual storages, as well as system overflows (Figure 6g,h), are provided.

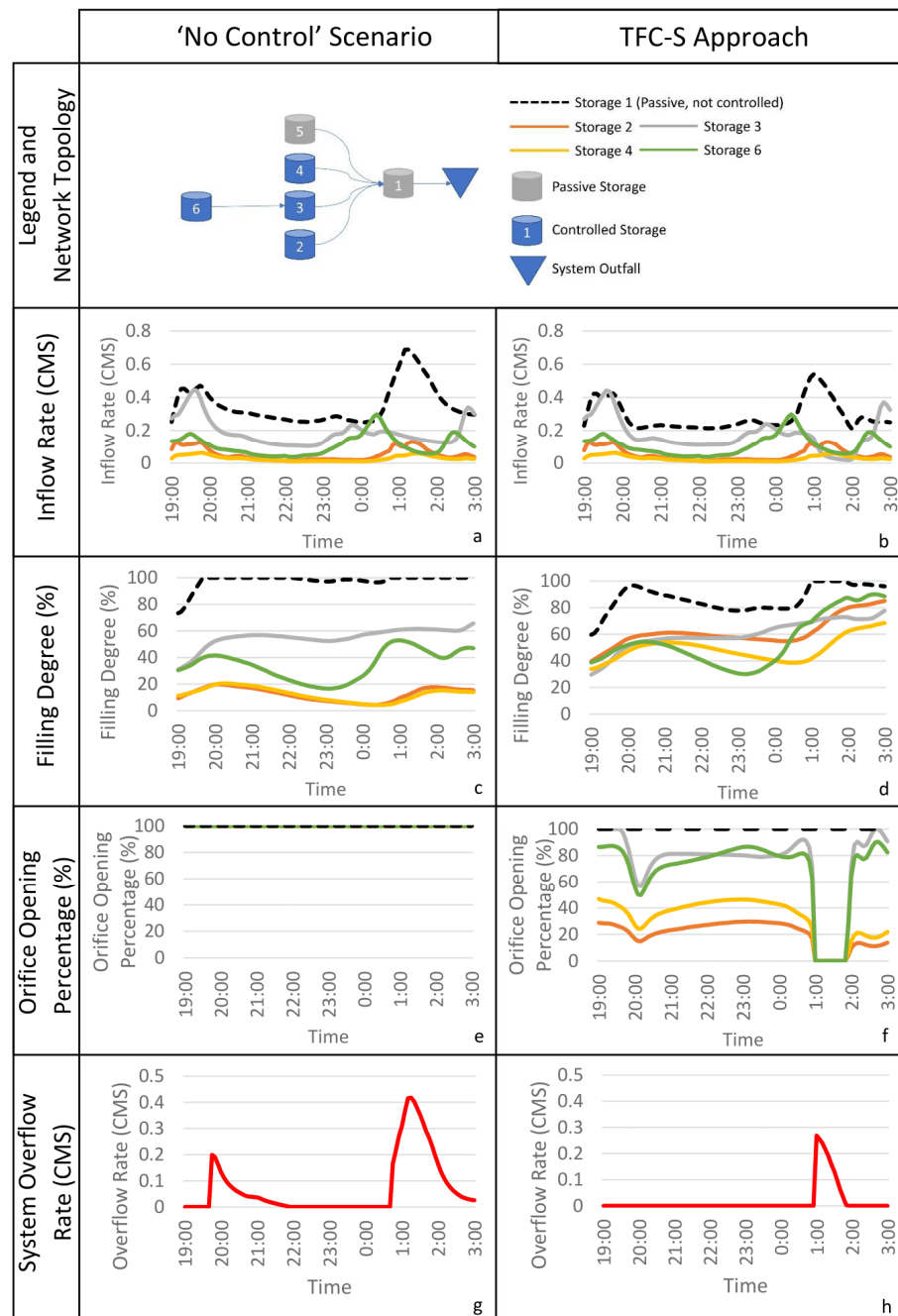


Figure 6. Comparison between the TFCS approach and 'No Control' scenario for the combined storage system of Case Study 2 for an example 8 h rainfall period (10 May 2000 19:00–11 May 2000 3:00). (a) shows the inflow rate over time for the 'no control' scenario, (b) shows the inflow rate over time for the TFC-S approach, (c) shows the filling degree over time for the 'no control' scenario, (d) shows the filling degree over time for the TFC-S approach, (e) shows the orifice opening percentage over time for the 'no control' scenario, (f) shows the orifice opening percentage over time for the TFC-S approach, (g) shows the system overflow rate over time for the 'no control' scenario, (h) shows the system overflow rate over time for the TFC-S approach. The network topology is show in the diagram at the top of the figure.

For this illustration, we choose an 8 h rainfall period from 10 May 2000 19:00 to 11 May 2000 03:00, as for this period, the system overflow volume (i.e., the objective of this case study) is reduced significantly with the aid of the TFCS approach compared with that obtained from the 'No Control' scenario (red line, Figure 6g,h). This is achieved by utilizing and approximately balancing the filling degree of storages in the system using the orifice equation (Equation (1)) and methods described in Section 2.1.

For the 'No Control' scenario, there are two system overflow events during the selected time period, including 1. a small volume event from 10 May 2000 19:45 to 10 May 2000 22:00, and 2. a large volume event from 11 May 2000 00:45 to 11 May 2000 03:00 (red line, Figure 6g). Between 10 May 2000 19:45 and 10 May 2000 20:00, there is a significant inflow peak for storage 1 (black dashed line, Figure 6a), and as a result, the filling degree of storage 1 increased rapidly to 100% at 10 May 2000 20:00 (black dashed line, Figure 6c), and the first overflow event starts (red line, Figure 6g). After 10 May 2000 20:00, the filling degree of storage 1 is always at a high level (close to 100%, black dashed line, Figure 6c), and the significant inflow peak that occurs from 11 May 2000 00:45 to 11 May 2000 02:00 (black dashed line, Figure 6a) leads to the second large volume overflow event. The inflow to storage 1 is contributed to by outflows from storages 2, 3, and 4. During the entire time period, the filling degrees of storages 2, 3, 4, and 6 are relatively low: less than 60% for storages 3 and 6 and less than 20% for storages 2 and 4 (Figure 6c), which indicates that there is unutilized storage capacity in the system when the significant overflow occurs at storage 1. For the 'No Control' scenario, this inefficient usage of storage capacity is due to the fact that all of the storages are equipped with passive orifices that are always fully open (100%, Figure 6e).

In comparison, for the proposed TFCS approach, there is only one system overflow event during the selected time period from 11 May 2000 01:00 to 11 May 2000 02:00 (red line, Figure 6h): the first small volume overflow event from the 'No Control' scenario is eliminated, and the second large volume overflow event is reduced significantly, with a 70% reduction in volume.

The reason for the elimination of the first volume event is that between 10 May 2000 19:00 and 10/5/2000 20:00, the orifice opening percentage of storages 2, 3, 4, and 6 decreases (Figure 6f) to limit the outflow from these upstream storages to deal with the increasing storage 1 filling degree, and, as a result, the inflow to storage 1 is reduced (black dashed line, Figure 6b). For example, at 10 May 2000 20:00, the inflow to storage 1 is reduced from $0.3 \text{ m}^3/\text{s}$ for the 'No Control' scenario (black dashed line, Figure 6a) to $0.2 \text{ m}^3/\text{s}$ (black dashed line, Figure 6b). With reduced inflow, the filling degree for storage 1 is capped at 98% (10 May 2000 20:00, black dashed line, Figure 6d), and the first small volume overflow event is mitigated.

The reason why the second volume event is reduced is that between 11 May 2000 01:00 and 11 May 2000 02:00, the orifices of storages 2, 3, 4, and 6 are fully closed (Figure 6f) to deal with the second large volume overflow event, and the inflow of storage 1 is clearly reduced for this time period (black dashed line, Figure 6a,b). Between 11 May 2000 01:00 and 11 May 2000 02:00, the peak inflow to storage 1 is reduced from $0.7 \text{ m}^3/\text{s}$ for the 'No Control' scenario (black dashed line, Figure 6a) to $0.52 \text{ m}^3/\text{s}$ (black dashed line, Figure 6b). Although the filling degree of storage 1 still reaches 100% at 11 May 2000 01:00 and overflows afterwards, the filling degrees of storages 2, 3, 4, and 6 are higher and more similar to each other (Figure 6d) than in the 'No Control' scenario (Figure 6c). For example, storage 2 filling degrees are generally less than 20% in the 'No Control' scenario when storage 1 is full and overflows (orange line, Figure 6c), while this number is increased to 60% with the TFCS approach (orange line, Figure 6d). Therefore, by using the TFCS approach, the storage capacity in the system is better utilized, and a significant reduction in overflow volume is achieved.

4.3. Summary of Results: Benchmarking Performance and Practicality of the TFCS Approach

Figure 7 summarises the performance and practicality of the TFCS approach compared to the ‘No Control’ scenario and benchmark RTC approaches, including the calibrated equal filling degree approach (calibrated EFD) and existing advanced approaches (reinforcement learning (RL) for Case Study 1, model predictive control (MPC) for Case Study 2 and optimized predictive control (OPC) for Case Study 3). Both quantitative performance and practicality are categorized into three groups (low/medium/high) for ease of comparison of the control approaches across multiple case studies with different performance measures and different levels of practicality.

Control Approach		Practicality	Performance				Overall
			CS 1: Time (%) ¹	CS2: Reduction(%) ²	CS 3: Time(%) ³	CS3: Deviation(m) ⁴	
No Control		High	47%	0%	76%	689m	Low
Calibrated EFD		Medium	7%	6.4%	38%	82m	Medium
Existing Advanced Approach	RL	Medium-Low	23%	-	-	-	Medium
	MPC	Low	-	13%	-	-	High
	OPC	Low	-	-	1.1%	0.1m	High
TFCS		High	0%	13%	3.2%	0.3m	High

Performance Measures:

1. Percentage of time exceeds the threshold
2. Percentage reduction of Total Overflow Volume
3. Percentage of Time Outside of the Operational Boundary
4. Total Deviation of Storage Level

Figure 7. Summary of performance and practicality of TFCS and benchmark RTC approaches (RL: reinforcement learning, MPC: model predictive control, OPC: optimized predictive control). The “green” cells correspond to a “High” level of performance, the “orange” cells correspond to a “Medium” level of performance and the “red” cells correspond to a “Low” level of performance of the different control algorithms considered relative to the ‘No Control’ scenario.

The performance classification of RTC approaches is determined by comparison with the ‘No Control’ scenario (no change—red, medium improvement—yellow, and high improvement—green).

For Case Study 1 (first column under ‘performance’, Figure 7), a ‘medium’ performance classification is assigned to the calibrated EFD (7% of time exceeding threshold) and the RL control approaches (23% of time exceeding threshold) because they both produce improved performance compared with that of the ‘No Control’ approach (47% of time exceeding threshold). The TFCS approach is assigned a ‘high’ performance classification because there is 0% of time exceeding the threshold, and it outperforms all other control approaches.

For Case Study 2 (second column under ‘performance’, Figure 7), the performance of the calibrated EFD approach (6.4% reduction in overflow volume) is classified as ‘medium’ as there is an improvement compared to the ‘No Control’ scenario (0% reduction in overflow volume). The performances of both the MPC and TFCS approaches are classified as ‘high’ as both are able to achieve a 13.2% reduction in overflow volume reduction, which is better than that of the calibrated EFD approach.

For Case Study 3 (third and fourth columns under ‘performance’, Figure 7), the calibrated EFD approach performance (37.5% of the time outside the operational boundary and 82 m total deviation of storage level) is classified as ‘medium’ because its performance is improved compared to that of the ‘No Control’ scenario (76% of the time outside the operational boundary and 689 m total deviation of storage level). The performances of both the OPC and TFCS approaches are classified as ‘high’ as their performance measures

(1.1–3.2% of the time outside the operational boundary and 0.1–0.3 m total deviation of storage level) are better than that of the calibrated EFD approach.

The ‘overall performance’ of different control approaches (fifth column under ‘performance’, Figure 7) is based on their performance across the three case studies, where available. The overall performances of the calibrated EFD and RL approaches are classified as ‘medium’ as they are better than that of the ‘No Control’ scenario. The performances of the MPC, OPC, and TFCS approaches are classified as ‘high’ as their performances are significantly better than those of the ‘No Control’ and calibrated EFD approaches.

The performances of the different control approaches described previously are achieved with various levels of practicality based on the information required to implement them (second column, Figure 7). Some control approaches require calibration with a large amount of data, while others require information of perfect rainfall forecast information. This ‘practicality’ of each control approach is divided into three categories: low, medium, and high. The ‘low’ classification (labelled in red, Figures 7 and 8) is for RTC approaches that require information that is difficult to obtain, such as perfect forecasts of future rainfall and/or high computational requirements. The ‘medium’ classification (labelled in yellow, Figures 7 and 8) is for control approaches that require a large amount of information, such as calibration with a large number of storms prior to being applied. The ‘high’ classification (labelled in green, Figures 7 and 8) is for RTC approaches that only use data that can be measured/accessed easily and have low computational requirements.

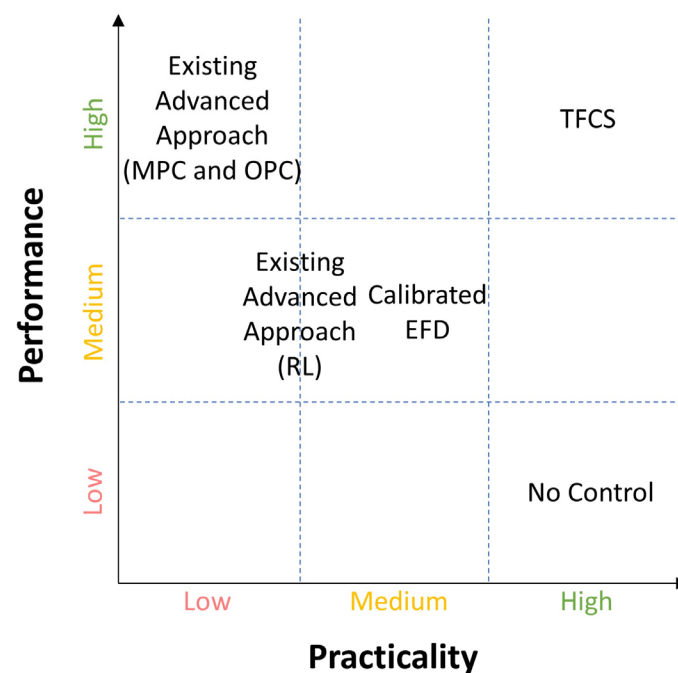


Figure 8. Mapping of the relationship between performance and practicality for the five RTC control approaches considered and the ‘No Control’ benchmark scenario.

The ‘No Control’ scenario is classified as having a ‘high’ level of practicality as no information is required. The TFCS approach is also classified as having a ‘high’ level of practicality as it only uses storage-level information that can be measured easily in real time with the aid of low-cost pressure sensors. The calibrated EFD approach is classified as having a ‘medium’ level of practicality as it requires calibration with a large amount of data. As a result, the limitations of calibration will impact the performance of the calibrated EFD approach, as the calibration will generally require manual or optimized tuning of parameters for specific conditions, which limits the ability of the calibrated EFD approach to be applied broadly and under changing conditions.

The practicality of both MPC and OPC approaches is classified as ‘low’, as they both require perfect knowledge of future rainfall forecasts. It is unlikely that perfect rainfall forecast at 5 min time intervals over long lead times will be available any time soon. In practical situations, the MPC and OPC approaches will need to utilize highly uncertain rainfall forecasts, which will reduce their performances in practice. In addition, both MPC and OPC approaches require extensive computational resources and effort to enable the control schemes to be optimized in real time for a short prediction window.

The level of practicality of the reinforcement learning (RL) approach is classified as ‘medium–low’ because it requires the preparation of extensive training datasets, followed by training of the controllers on these prepared datasets, which requires high computational resources such as GPUs. Therefore, although the level of practicality of the RL approach is higher than that of the OPC and MPC approaches as it does not rely on perfect rainfall information, its practicality is still lower than that of the calibrated EFD and TFCS approaches due to the high requirement of computational resources.

Figure 8 maps the performance and practicality categorization of the five RTC control approaches analysed in this study along with that of the ‘No Control’ benchmark approach. The ‘No Control’ approach has a ‘high’ level of practicality with a ‘low’ overall performance. The calibrated EFD approach has a ‘medium’ level of both practicality and performance. The MPC and OPC approaches have ‘high’ performance. However, they have a ‘low’ level of practicality due to their dependency on perfect forecasting of future rainfall. The RL approach has a ‘medium’ level of performance with a ‘low–medium’ level of practicality due to its requirements of high computational resources. The proposed TFCS approach is the only one of the five RTC control approaches analysed that has both ‘high’ overall performance and a ‘high’ level of practicality, which means that it performs well and is broadly applicable to a wide range of case studies.

5. Discussion

5.1. Practical Benefits of the TFCS Approach

There are a number of practical benefits to applying the proposed TFCS approach to existing stormwater storage systems. Firstly, by utilizing existing storage capacity, the TFCS approach is able to extend the lifespan of storage systems and delay the need for stormwater conveyance infrastructure system upgrades for as long as possible. Secondly, this approach can be adapted to climate change and land use change. The TFCS approach only requires knowledge of the desired outflow from a storage, as well as storage-level information that can be easily measured in real time with the aid of low-cost pressure sensors, which allows it to be ‘calibration free’. This makes it suitable to deal with catchments that are subject to changing conditions. Thirdly, this approach can be adapted to achieve a number of stormwater management objectives, including improving water quality and stormwater harvesting. For example, by introducing retention capacity for intercepting runoff from impervious surfaces, water quality can be improved [36]. During drought periods, the storage outlet could be closed to harvest stormwater for environmental purposes [37], and the stormwater storage can be integrated with bioretention systems to improve downstream water quality [38].

5.2. Practicality of Implementation

With the aid of low-cost pressure sensors, the required storage levels can be easily measured in real time, and, as a result, the outlet orifices of stormwater storages can be adjusted accordingly to maximize the utilization of the available storage capacity. Using current technology, an electric actuator can be used to adjust the position of a valve from fully closed to fully open in a short period of time [39,40]. Hence, any control time steps longer than 5 min are achievable from a practical perspective.

5.3. Future Research

Future research should be undertaken to (i) test the performance and practicality of the proposed approach under a wider range of conditions, such as under different climate and land use change scenarios [41,42], (ii) extend the approach to cater to catchment inflows (see Section 2.2), (iii) assess the impact of the assumption of small travel times (see Section 2.2) on the performance of the TFCS approach for systems covering larger spatial extents [43], (iv) assess whether the addition of smart controls to storages is likely to result in any additional risks (e.g., cyber risks [44]), (v) develop a framework to identify the required storage volume for specific design rainfall events, and (vi) demonstrate the practicality of the proposed approach with the aid of physical experiments in the laboratory or in full-scale field tests.

6. Conclusions

This study introduces the target flow control systems (TFCS) approach, which extends the TFC approach of Liang et al. (2022) [17] so that it is applicable to systems of storages that are controlled to achieve desired flow conditions at locations of interest. This is achieved by determining the target outflows of individual storages based on the storage-level information measured in real time and knowledge of the desired maximum flow at critical points in the downstream infrastructure. The individual storage orifice opening percentages are then adjusted with the aid of the orifice equation and storage-level information to achieve the individual targets.

The utility of the proposed TFCS approach was compared with that of five control approaches (two common benchmark control approaches, including ‘No Control’ and ‘calibrated EFD’, and three existing advanced control approaches from the literature, including ‘reinforcement learning’, ‘model predictive control’, and ‘optimized predictive control’) for three case studies from the literature with different configurations and stormwater management objectives. Results show that the TFCS approach is the only one of the five RTC control approaches analysed that has both ‘high’ overall performance and a ‘high’ level of practicality, which means that it performs well and is also broadly applicable to a wide range of case studies. This is because the TFCS approach does not require calibration to specific local conditions and only relies on real-time storage-level information. In addition, the calibration-free nature of the proposed TFCS approach enables it to be applied to a wide range of catchments and adapt to changes in land use and climate. Consequently, the TFCS approach has the potential to maximize utilization of the capacity of existing stormwater systems for achieving multiple stormwater management objectives, which could potentially avoid costly upgrades.

Future research should assess the proposed TFCS approach across a wider range of conditions, including various climate change scenarios, and to incorporate catchment inflows. Additionally, a framework for estimating required storage volumes for specific design rainfall events should be developed. Finally, the practicality of the approach should be validated through both laboratory experiments and full-scale field tests.

Author Contributions: All authors conceived and designed the experiments. R.L. performed the experiments. All authors analysed the data. All authors contributed to writing the paper. All authors have read and agreed to the published version of the manuscript.

Funding: This research received no external funding. Ruijie Liang received a scholarship provided by the University of Adelaide.

Data Availability Statement: The data presented in this study are openly available in Open Science Framework (OSF) at <https://osf.io/dbynw/>, DOI = DOI 10.17605/OSF.IO/DBYNW.

Acknowledgments: The authors would like to thank the two anonymous reviewers, whose comments have assisted us with improving the quality of the paper.

Conflicts of Interest: The authors declare no conflicts of interest.

Appendix A

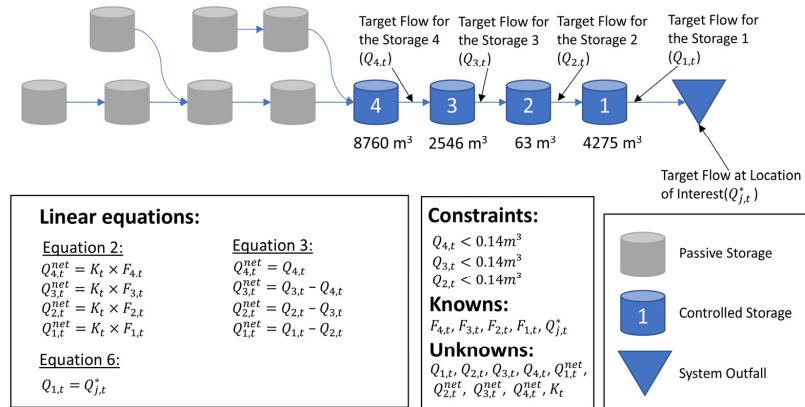


Figure A1. Formulation of Case Study 1.

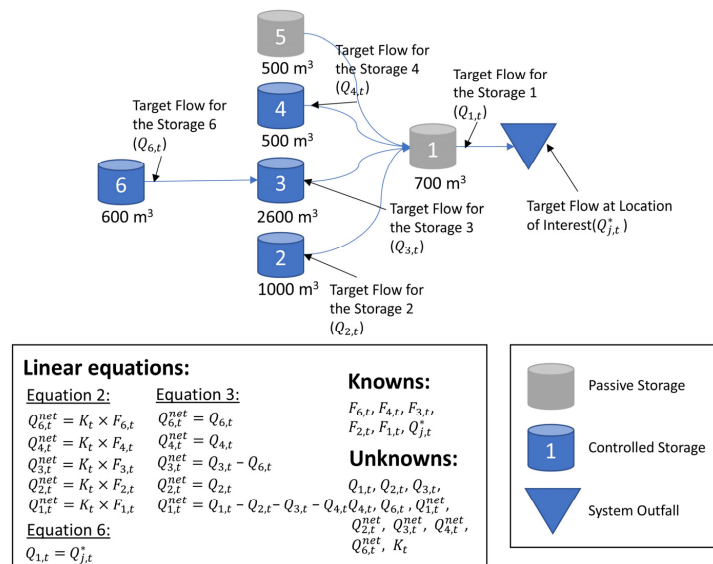


Figure A2. Formulation of Case Study 2.

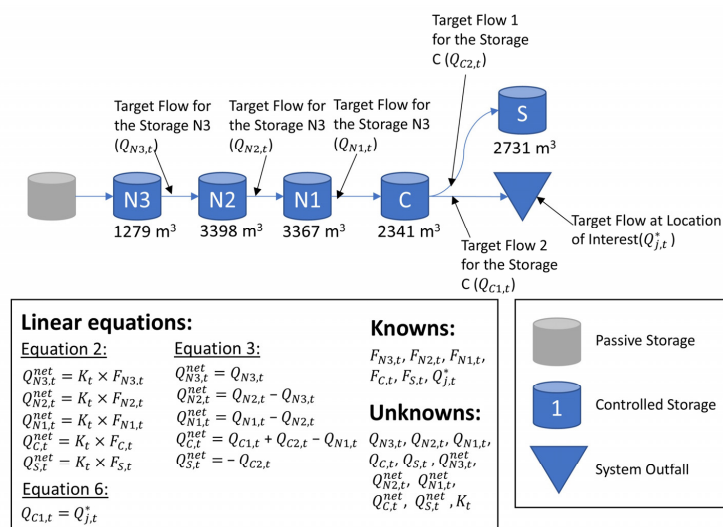


Figure A3. Formulation of Case Study 3.

References

1. Campisano, A.; Butler, D.; Ward, S.; Burns, M.J.; Friedler, E.; DeBusk, K.; Fisher-Jeffes, L.N.; Ghisi, E.; Rahman, A.; Furumai, H. Urban rainwater harvesting systems: Research, implementation and future perspectives. *Water Res.* **2017**, *115*, 195–209. [[CrossRef](#)] [[PubMed](#)]
2. Shishegar, S.; Duchesne, S.; Pelletier, G. Optimization methods applied to stormwater management problems: A review. *Urban Water J.* **2018**, *15*, 276–286. [[CrossRef](#)]
3. Liang, R.; Di Matteo, M.; Maier, H.R.; Thyer, M.A. Real-Time, Smart Rainwater Storage Systems: Potential Solution to Mitigate Urban Flooding. *Water* **2019**, *11*, 2428. [[CrossRef](#)]
4. Locatelli, L.; Mark, O.; Mikkelsen, P.S.; Arnbjerg-Nielsen, K.; Deletic, A.; Roldin, M.; Binning, P.J. Hydrologic impact of urbanization with extensive stormwater infiltration. *J. Hydrol.* **2017**, *544*, 524–537. [[CrossRef](#)]
5. Van der Bruggen, B.; Borghgraef, K.; Vinckier, C. Causes of water supply problems in urbanised regions in developing countries. *Water Resour. Manag.* **2010**, *24*, 1885–1902. [[CrossRef](#)]
6. Lund, N.S.V.; Falk, A.K.V.; Borup, M.; Madsen, H.; Steen Mikkelsen, P. Model predictive control of urban drainage systems: A review and perspective towards smart real-time water management. *Crit. Rev. Environ. Sci. Technol.* **2018**, *48*, 279–339. [[CrossRef](#)]
7. Di Matteo, M.; Liang, R.; Maier, H.R.; Thyer, M.A.; Simpson, A.R.; Dandy, G.C.; Ernst, B. Controlling rainwater storage as a system: An opportunity to reduce urban flood peaks for rare, long duration storms. *Environ. Model. Softw.* **2019**, *111*, 34–41. [[CrossRef](#)]
8. Liang, R.; Thyer, M.A.; Maier, H.R.; Dandy, G.C.; Di Matteo, M. Optimising the design and real-time operation of systems of distributed stormwater storages to reduce urban flooding at the catchment scale. *J. Hydrol.* **2021**, *602*, 126787. [[CrossRef](#)]
9. Li, J. A data-driven improved fuzzy logic control optimization-simulation tool for reducing flooding volume at downstream urban drainage systems. *Sci. Total Environ.* **2020**, *732*, 138931. [[CrossRef](#)]
10. Meneses, E.J.; Gaussens, M.; Jakobsen, C.; Mikkelsen, P.S.; Grum, M.; Vezzaro, L. Coordinating rule-based and system-wide model predictive control strategies to reduce storage expansion of combined urban drainage systems: The case study of Lundtofte, Denmark. *Water* **2018**, *10*, 76. [[CrossRef](#)]
11. Sharior, S.; McDonald, W.; Parolari, A.J. Improved reliability of stormwater detention basin performance through water quality data-informed real-time control. *J. Hydrol.* **2019**, *573*, 422–431. [[CrossRef](#)]
12. Ibrahim, Y.A. Real-Time Control Algorithm for Enhancing Operation of Network of Stormwater Management Facilities. *J. Hydrol. Eng.* **2020**, *25*, 04019065. [[CrossRef](#)]
13. Schmitt, Z.K.; Hodges, C.C.; Dymond, R.L. Simulation and assessment of long-term stormwater basin performance under real-time control retrofits. *Urban Water J.* **2020**, *17*, 467–480. [[CrossRef](#)]
14. Dong, X.; Huang, S.; Zeng, S. Design and evaluation of control strategies in urban drainage systems in Kunming city. *Front. Environ. Sci. Eng.* **2017**, *11*, 1–8. [[CrossRef](#)]
15. Muschalla, D.; Vallet, B.; Anctil, F.; Lessard, P.; Pelletier, G.; Vanrolleghem, P.A. Ecohydraulic-driven real-time control of stormwater basins. *J. Hydrol.* **2014**, *511*, 82–91. [[CrossRef](#)]
16. Sadler, J.M.; Goodall, J.L.; Behl, M.; Bowes, B.D.; Morsy, M.M. Exploring real-time control of stormwater systems for mitigating flood risk due to sea level rise. *J. Hydrol.* **2020**, *583*, 124571. [[CrossRef](#)]
17. Liang, R.; Maier, H.R.; Thyer, M.A.; Dandy, G.C.; Tan, Y.; Chhay, M.; Sau, T.; Lam, V. Calibration-free approach to reactive real-time control of stormwater storages. *J. Hydrol.* **2022**, *614*, 128559. [[CrossRef](#)]
18. Mullapudi, A.; Lewis, M.J.; Gruden, C.L.; Kerkez, B. Deep reinforcement learning for the real time control of stormwater systems. *Adv. Water Resour.* **2020**, *140*, 103600. [[CrossRef](#)]
19. Sun, C.; Lorenz Svendsen, J.; Borup, M.; Puig, V.; Cembrano, G.; Vezzaro, L. An MPC-enabled SWMM implementation of the Astlingen RTC benchmarking network. *Water* **2020**, *12*, 1034. [[CrossRef](#)]
20. Rimer, S.P.; Mullapudi, A.; Troutman, S.C.; Ewing, G.; Bowes, B.D.; Akin, A.A.; Sadler, J.; Kertesz, R.; McDonnell, B.; Montestruque, L. pystorms: A simulation sandbox for the development and evaluation of stormwater control algorithms. *Environ. Model. Softw.* **2023**, *162*, 105635. [[CrossRef](#)]
21. Schütze, M.; Lange, M.; Pabst, M.; Haas, U. Astlingen—a benchmark for real time control (RTC). *Water Sci. Technol.* **2018**, *2017*, 552–560. [[CrossRef](#)] [[PubMed](#)]
22. Reader-Harris, M.; Sattary, J. The orifice plate discharge coefficient equation. *Flow Meas. Instrum.* **1990**, *1*, 67–76. [[CrossRef](#)]
23. Reader-Harris, M.; Sattary, J.; Spearman, E. The orifice plate discharge coefficient equation—Further work. *Flow Meas. Instrum.* **1995**, *6*, 101–114. [[CrossRef](#)]
24. Borsanyi, P.; Benedetti, L.; Dirckx, G.; De Keyser, W.; Muschalla, D.; Solvi, A.-M.; Vandenberghe, V.; Weyand, M.; Vanrolleghem, P.A. Modelling real-time control options on virtual sewer systems. *J. Environ. Eng. Sci.* **2008**, *7*, 395–410. [[CrossRef](#)]
25. Dirckx, G.; Schütze, M.; Kroll, S.; Thoeye, C.; De Guedre, G.; Van De Steene, B. Cost-efficiency of RTC for CSO impact mitigation. *Urban Water J.* **2011**, *8*, 367–377. [[CrossRef](#)]
26. Wang, P.; Mou, S.; Lian, J.; Ren, W. Solving a system of linear equations: From centralized to distributed algorithms. *Annu. Rev. Control* **2019**, *47*, 306–322. [[CrossRef](#)]
27. Hackbusch, W. *Iterative Solution of Large Sparse Systems of Equations*; Springer: Berlin/Heidelberg, Germany, 1994; Volume 95. [[CrossRef](#)]
28. Rutishauser, H. The Jacobi method for real symmetric matrices. *Numer. Math.* **1966**, *9*, 1–10. [[CrossRef](#)]

29. Maier, H.R.; Razavi, S.; Kapelan, Z.; Matott, L.S.; Kasprzyk, J.; Tolson, B.A. Introductory overview: Optimization using evolutionary algorithms and other metaheuristics. *Environ. Model. Softw.* **2019**, *114*, 195–213. [[CrossRef](#)]
30. Gironás, J.; Roesner, L.A.; Rossman, L.A.; Davis, J. A new applications manual for the Storm Water Management Model(SWMM). *Environ. Model. Softw.* **2010**, *25*, 813–814. [[CrossRef](#)]
31. Fortin, F.-A.; De Rainville, F.-M.; Gardner, M.-A.G.; Parizeau, M.; Gagné, C. DEAP: Evolutionary algorithms made easy. *J. Mach. Learn. Res.* **2012**, *13*, 2171–2175. [[CrossRef](#)]
32. Auger, A.; Bader, J.; Brockhoff, D.; Zitzler, E. Theory of the hypervolume indicator: Optimal μ -distributions and the choice of the reference point. In Proceedings of the Tenth ACM SIGEVO Workshop on Foundations of Genetic Algorithms, Orlando, FL, USA, 9–11 January 2009; pp. 87–102. [[CrossRef](#)]
33. Beume, N.; Naujoks, B.; Emmerich, M. SMS-EMOA: Multiobjective selection based on dominated hypervolume. *Eur. J. Oper. Res.* **2007**, *181*, 1653–1669. [[CrossRef](#)]
34. Zitzler, E.; Brockhoff, D.; Thiele, L. The hypervolume indicator revisited: On the design of Pareto-compliant indicators via weighted integration. In Proceedings of the International Conference on Evolutionary Multi-Criterion Optimization, Matsushima, Japan, 5–8 March 2007; pp. 862–876. [[CrossRef](#)]
35. McDonnell, B.E.; Ratliff, K.; Tryby, M.E.; Wu, J.J.X.; Mullapudi, A. PySWMM: The Python Interface to Stormwater Management Model (SWMM). *J. Open Source Softw.* **2020**, *5*, 2292. [[CrossRef](#)] [[PubMed](#)]
36. Walsh, C.J.; Imberger, M.; Burns, M.J.; Bos, D.G.; Fletcher, T.D. Dispersed Urban-Stormwater Control Improved Stream Water Quality in a Catchment-Scale Experiment. *Water Resour. Res.* **2022**, *58*, e2022WR032041. [[CrossRef](#)]
37. Xu, W.D.; Burns, M.J.; Cherqui, F.; Duchesne, S.; Pelletier, G.; Fletcher, T.D. Real-time controlled rainwater harvesting systems can improve the performance of stormwater networks. *J. Hydrol.* **2022**, *614*, 128503. [[CrossRef](#)]
38. de Macedo, M.B.; do Lago, C.A.F.; Mendiola, E.M. Stormwater volume reduction and water quality improvement by bioretention: Potentials and challenges for water security in a subtropical catchment. *Sci. Total Environ.* **2019**, *647*, 923–931. [[CrossRef](#)] [[PubMed](#)]
39. Cui, B.; Lin, Z.; Zhu, Z.; Wang, H.; Ma, G. Influence of opening and closing process of ball valve on external performance and internal flow characteristics. *Exp. Therm. Fluid Sci.* **2017**, *80*, 193–202. [[CrossRef](#)]
40. Ma, G.; Lin, Z.; Zhu, Z.; Fang, Y. Effect of variable speed motion curve of electric actuator on ball valve performance and internal flow field. *Adv. Mech. Eng.* **2021**, *13*, 16878140211028003. [[CrossRef](#)]
41. Fowler, K.J.A.; McMahon, T.A.; Westra, S.; Horne, A.; Guillaume, J.H.A.; Guo, D.; Nathan, R.; Maier, H.R.; John, A. Climate stress testing for water systems: Review and guide for applications. *WIREs Water* **2024**, e1747. [[CrossRef](#)]
42. Hamers, E.; Maier, H.R.; Zecchin, A.C.; van Delden, H. Framework for considering the interactions between climate change, socio-economic development and land use planning in the assessment of future flood risk. *Environ. Model. Softw.* **2024**, *171*, 105886. [[CrossRef](#)]
43. Hamers, E.; Maier, H.R.; Zecchin, A.C.; van Delden, H. Effectiveness of nature-based solutions for mitigating the impact of pluvial flooding in urban areas at the regional scale. *Water* **2023**, *15*, 642. [[CrossRef](#)]
44. Keenan, C.; Maier, H.R.; van Delden, H.; Zecchin, A.C. Bridging the cyber-physical divide: A novel approach for quantifying and visualising the cyber risk of physical assets. *Water* **2024**, *16*, 637. [[CrossRef](#)]

Disclaimer/Publisher’s Note: The statements, opinions and data contained in all publications are solely those of the individual author(s) and contributor(s) and not of MDPI and/or the editor(s). MDPI and/or the editor(s) disclaim responsibility for any injury to people or property resulting from any ideas, methods, instructions or products referred to in the content.